Conformations of Nucleotides Bound to Wild Type and Y78F Mutant Yeast Guanylate Kinase: Proton Two-Dimensional Transferred NOESY Measurements†

Bruce D. Ray,‡ Gotam K. Jarori,‡,§ Vidya Raghunathan,‡,|| Honggao Yan,⊥ and B. D. Nageswara Rao*,‡

Department of Physics, Indiana University-Purdue University at Indianapolis (IUPUI), 402 North Blackford Street, Indianapolis, Indiana 46202-3273, and Department of Biochemistry and Molecular Biology, Michigan State University, East Lansing, Michigan 48824

Received May 16, 2005; Revised Manuscript Received July 20, 2005

ABSTRACT: Wild type and Y78F mutant yeast guanylate kinase (GKy) were studied to investigate the effects of a site-directed mutation on bound substrate conformations. Previously published work showed that Y78 is involved in GMP binding and that the Y78F mutant has 30-fold weaker GMP binding and 2 orders of magnitude less activity, than the wild type. Adenosine conformations of adenosine 5′-triphosphate (ATP) and adenosine 5′-diphosphate (ADP) and guanosine conformations of guanosine 5′-monophosphate (GMP) bound to wild type and Y78F mutant yeast guanylate kinase in the complexes GKy·Mg(II)ATP, GKy·Mg(II)ADP, GKy·GMP, and GKy·Mg(II)ADP·[U-^{13}C]GMP were determined by two-dimensional transferred nuclear Overhauser effect (TRNOESY) measurements combined with molecular dynamics simulations. For adenyl nucleotides in wild type complexes, all glycosidic torsion angles, χ, were 54 ± 5°. In Y78F mutant complexes, adenyl nucleotide glycosidic torsion angles were 55 ± 5° (GKy·MgATP) and 49 ± 5° (GKy·MgADP). Thus, the adenyl nucleotides bind similarly for both the wild type and Y78F mutant complexes. However, in the fully constrained, two-substrate complexes, GKy·Mg(II)ADP·[U-^{13}C]GMP, the guanyl glycosidic torsion angle, χ, is 50 ± 5° with the wild type and 83 ± 5° with the Y78F mutant. This difference suggests that an unfavorable torsion may be a large part of the mechanism for significantly weaker GMP binding to reaction complexes of the Y78F mutant.

It is generally accepted that knowledge of a productive conformational arrangement of enzyme-bound substrates and their amino acid environment is a prerequisite for elucidating the molecular basis of enzyme catalysis. In a bisubstrate reaction, the productive conformations may be characterized in terms of their structural features, viz., (i) the relative orientation of the moieties within each bound substrate, (ii) the relative orientation of bound substrates with respect to each other, (iii) the orientation of each bound substrate with respect to the critical moieties of the enzyme, (iv) the catalytic moieties themselves, (v) the distances of traversal by the itinerant moieties, and (vi) the attendant structural alterations in the remaining parts of substrates. Site-directed mutagenesis may be used to elucidate these interactions provided that all of these factors can be taken into account. Typically, however, site-directed mutagenesis studies of enzyme mechanisms are based on kinetic and binding constant measurements. The conclusions reached from these studies implicitly presume that the mutation leaves the various critical structural elements and the traversal distances unaffected. It may be argued on general grounds that such an assumption is not likely to be universally valid. Structure determinations using mutated enzymes, aimed at validating the presumed retention of gross conformation of enzyme-bound reaction complexes, are required to resolve this question. This paper presents some results of such structural measurements of enzyme-bound substrate complexes of wild type and Y78F mutant forms of yeast guanylate kinase by high-resolution NMR.[1] NMR has been proven to be a useful experimental technique for the determination of bound substrate conformations and distances of traversal of itinerant moieties in solution phase (*1*−*6*, *38*, *39*).

Guanylate kinase (GK) is a small, typically monomeric enzyme that catalyzes the reversible reaction

$$\mathrm{MgATP} + \mathrm{GMP} \leftrightarrow \mathrm{MgADP} + \mathrm{GDP} \qquad (1)$$

which is similar to the adenylate kinase reaction (*7*, *8*). Because the enzyme is essential for conversion of GMP to GDP, it plays an important role in GTP biosynthesis. Consequently, it plays a role in those cellular functions that involve GTP such as the control of the cGMP cycle (*9*).

† Supported in part by National Institutes of Health (Grant GM43966) and IUPUI.

* To whom correspondence should be addressed. Phone: (317) 274-6897. Fax: (317) 274-2393. E-mail: brao@iupui.edu.

‡ Indiana University-Purdue University at Indianapolis.

§ Permanent address: Tata Institute of Fundamental Research, Mumbai, India.

|| Permanent address: National Institute of Immunology, New Delhi, India.

⊥ Michigan State University.

[1] Abbreviations: 2D, two-dimensional; ADP, adenosine 5′-diphosphate; ADP, adenosine 5′-diphosphate; ATP, adenosine 5′-triphosphate; GK, guanylate kinase; GKy, cloned yeast guanylate kinase; GMP, guanosine 5′-monophosphate; MD, molecular dynamics; NMR, nuclear magnetic resonance; nOe, nuclear Overhauser effect; PDB, Protein Data Bank; rmsd, root-mean-square deviation; Tris-d_{11}, deuterated tris-(hydroxymethyl)aminomethane; TRNOESY, transferred two-dimensional nuclear Overhauser effect spectroscopy.

10.1021/bi0509088 CCC: $30.25
Published on Web 09/29/2005

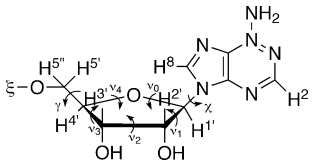

FIGURE 1: Chemical structure of the adenosine moiety showing the numbering for the relevant protons and the torsion angles. Torsions are denoted as follows: χ (O4′−C1′−N9−C8), ν_0 (C4′−O4′−C1′−C2′), ν_1 (O4′−C1′−C2′−C3′), ν_2 (C1′−C2′−C3′−C4′), ν_3 (C2′−C3′−C4′−O4′), ν_4 (C3′−C4′−O4′−C1′), and γ (O5′−C5′−C4′−C3′).

Because of its role in GTP biosynthesis, GK participates in the activation of antiviral acyclic guanosine analogues (*10*−*12*). Interestingly, several cell membrane-associated proteins have domains that are significantly homologous in sequence to GK (*13*−*16*). The crystal structure of the yeast GKy·GMP complex has been determined to 2 Å resolution (*17*, *18*) and compared to the apo-GKy and GKy·GMP crystal structures derived from the *Escherichia coli* expression of cloned recombinant yeast GK, which lacks N-terminal acetylation (*19*).

Despite the structural data given above, X-ray crystallographic information about the conformation of enzyme-bound substrates of GK remains scant. Thus far, crystals of GK with bound ATP or bound MgATP have not been obtained. As was the case with adenylate kinase, information regarding the ATP binding domain and evidence for any substrate binding-induced movements of this domain are inferred from crystal structure differences between crystals of the GKy apoenzyme and those of GKy with a nucleotide binding domain occupied by GMP.

Activity of the Y78F GKy mutant is decreased by a factor of >100 compared to that of the wild type (*20*). Furthermore, the mutation causes a greater than 20-fold weaker GMP K_m and greater than 10-fold weaker GMP K_d without significant effects on MgATP or MgADP binding, which suggests that the mutation site is strongly related to GMP binding (*20*). A comparison of the bound nucleotide conformations of the mutant with those of the wild type enzyme will address the question of the effect of the site-directed mutagenesis on the reaction complex structures.

In the case of enzymes for which nucleotides are substrates, the conformations of bound nucleotides are best determined by using two NMR methods: (i) proton TRNOESY measurements to determine nucleotide base and ribose conformations (*1*−*6*) and (ii) distance measurements on the basis of enhancement of spin relaxation rates of substrate nuclei, such as ^{31}P and ^{13}C, due to activating substituent paramagnetic cations (*38*, *39*). Specifically for ATP-utilizing enzymes, the NMR-determined nucleotide structures often exhibit subtle but unmistakable differences with respect to those determined by X-ray crystallography (*6*, *38*). These differences are large enough to make a significant impact on the description of the enzyme mechanism. For example, the glycosidic orientations in several ATP-utilizing enzymes, characterized by torsion angle χ (see Figure 1), as measured in solution by TRNOESY (*1*−*6*), cluster in a narrow range of 52 ± 8° (*4*, *6*). In contrast, glycosidic orientations measured from X-ray structures show a much greater variability (from −10° to 110°, with outliers between 170° and 180°, and from −130° to −170°) even for similar complexes with the same enzyme (*6*). This suggests that crystallization conditions play a role in redefining a bound nucleotide's orientation in an X-ray structure from a preferred productive orientation found in solution.

This paper presents TRNOESY-measured glycosidic orientations and sugar puckers for ATP, ADP, and GMP in wild type and Y78F mutant GKy complexes, E·MgATP, E·MgADP, and E·MgADP·GMP. Because of resonance overlaps both with the protein and between the nucleotides in the E·MgADP·GMP complex, a ^{13}C-selected nOe technique was used with [U-^{13}C]GMP to measure GMP TRNOESY spectra. This isotope-selective method can also be used to determine nOe's that cannot be measured because of overlapping protein resonances. In all complexes studied, concentrations of enzymes and substrates were optimized to minimize weak, nonspecific binding of nucleotides which often plagued early TRNOE measurements on ATP-utilizing enzymes (*1*).

EXPERIMENTAL PROCEDURES

Materials. GMP, ADP, ATP, tris(hydroxymethyl)aminomethane, and Sephadex G-75 were purchased from Sigma Chemical Co. DEAE-cellulose was from Whatman, Blue Sepharose resin from Pharmacia, Hepes from Research Organics, and Chelex-100 from Bio-Rad. Deuterated tris(hydroxymethyl)aminomethane (Tris-d_{11}), 99.96% D_2O, and sodium [2,2,3,3-D_4]trimethylsilylpropionate (TMSP) were from Cambridge Isotope Labs. All other chemicals were reagent grade.

Sample Preparation. Preparation of expression systems and purification for both wild type and Y78F mutant yeast GKy's have been performed according to previously published procedures (*8*, *20*), except that the Y78F mutant was eluted from the Blue Sepharose column with 30 mM Tris-HCl and 0.75 M KCl (pH 7.5). To further reduce adenylate kinase contamination, the resultant enzyme solutions were passed over DEAE-cellulose equilibrated with 30 mM Tris-HCl (pH 7.5) to which adenylate kinase binds and GKy does not (*7*). Enzyme purities were assessed by electrophoresis and specific activities were assayed by monitoring ADP and GDP formation in a coupled assay with pyruvate kinase and lactate dehydrogenase (*7*, *8*, *20*, *21*). At room temperature, the specific activity is typically 400 units/mg for the wild type and 2 units/mg for the Y78F mutant.

Enzyme solutions were prepared for TRNOESY by concentrating the enzyme to ∼100 mg/mL in an Amicon ultrafiltration concentrator with a YM10 membrane (molecular weight cutoff of 10 000) and exchanging the buffer with 30 mM Tris-d_{11} and 150 mM KCl (pH 7.5) in D_2O by repeated concentrations in a 3 mL Amicon concentrator. Nucleotides were prepared by dissolving the samples in D_2O, adjusting the pH to 8.0, and passing them through a Chelex-100 column to remove contaminating metal ions. Nucleotide solutions were then lyophilized, redissolved in D_2O, and stored at −20 °C until they were needed. Concentrations of nucleotides and enzymes were determined spectrophotometrically with the following extinction coefficients: $\epsilon_{259}^{mM} = 15.4\ cm^{-1}$ for ADP and ATP, $\epsilon_{252}^{mM} = 13.8\ cm^{-1}$ for GMP, and $\epsilon_{280}^{mg/mL} = 0.741\ cm^{-1}$ for both mutant and wild type GKy (molecular mass of 20 550 Da) (*8*, *20*). All buffer solutions were passed through Chelex-100 to remove trace

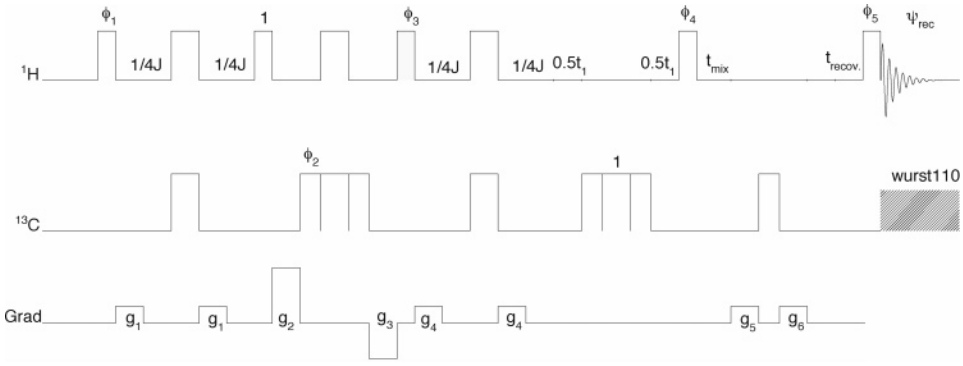

FIGURE 2: Pulse sequence of the gradient coherence-selected ^{13}C HSQC-NOESY used for ^{13}C selected TRNOESY. Pulses without indicated phases are phase *X*; $\varphi_1 = 4\ X, 4\ -X$; $\varphi_2 = 8\ X, 8\ -X$; $\varphi_3 = X, Y, -X, -Y$; $\varphi_4 = Y, X$; $\varphi_5 = -X, -Y$; and $\psi_{rec} = X, -Y, -X, Y, -X, Y, X, -Y, -X, Y, X, -Y, X, -Y, -X, Y$. States−TPPI for the ^{13}C-selected NOESY was achieved by incrementing φ_3 and ψ_{rec}. Processing coefficients were −1, 0, 0, 0, 0, −1, and 0. Gradients in gauss per centimeter were as follows: g_1, 4.8, 1 ms; g_2, 30.0, 4 ms; g_3, −19.3, 3 ms; g_4, 8.6, 1 ms; g_5, 3.2, 3 ms; and g_6 5.4, 5 ms.

metal ion impurities, and pH values were not corrected for D_2O isotope effects.

NMR Measurements. All TRNOESY experiments were performed at 5 °C on a Varian Inova-500 NMR spectrometer at the IUPUI NMR Center. A typical sample composition was 3 mM nucleotide and 0.3 mM GKy in a total volume of 700 μL. For experiments with Mg(II)-chelated nucleotides, Mg(II) was added as $MgCl_2$ in D_2O to give 7 mM Mg(II) to ensure complete saturation.

NOESY data were acquired in hypercomplex mode (*22*) with 2K (t_2) × 256 (t_1) complex data points for mixing times from 30 to 200 ms. For each t_1 increment, 16 scans and a relaxation delay of 2 s were used. Zero quantum interference was suppressed by random variation of the mixing time up to 10% of its value between different t_1 increments (*23*). In all experiments, the carrier frequency was placed 2 Hz to low field of the HDO resonance, and the solvent resonance was suppressed by monochromatic irradiation using the decoupler channel during the relaxation delay, t_1, and mixing periods. Data points were extended by linear prediction in both dimensions followed by Gaussian apodizations to give 4K (F_2) × 1K (F_1) complex point transformed data sets.

As stated in the introductory section, in preliminary experiments performed to obtain GMP conformation data for the E·MgADP·GMP complex, GMP and ADP sugar resonances overlapped. ^{13}C-selected NOESY with [U-^{13}C]-GMP overcomes this difficulty because only those protons directly bound to ^{13}C are able to transfer magnetization to other protons. Figure 2 shows the gradient coherence-selected ^{13}C HSQC-NOESY pulse sequence used for ^{13}C-selected NOESY. Figure 3 shows a typical ^{13}C-selected TRNOESY pattern for the E·MgADP·[U-^{13}C]GMP complex acquired with this pulse sequence. Previously, Wagner and Berger (*24*) published a slightly different pulse sequence for ^{13}C gradient-selected NOESY. Gradient coherence-selected ^{13}C HSQC-NOESY data were acquired in hypercomplex mode (*22*) with 2K (t_2) × 128 (t_1) complex data points for mixing times from 30 to 200 ms and without any further efforts to suppress either zero quantum interference or the solvent resonance. In these experiments, the carrier frequency was placed exactly on the HDO resonance, and 32 scans were recorded at each t_1 increment with a relaxation delay of 1 s. These data points were also extended by linear prediction in both dimensions followed by Gaussian apodizations to

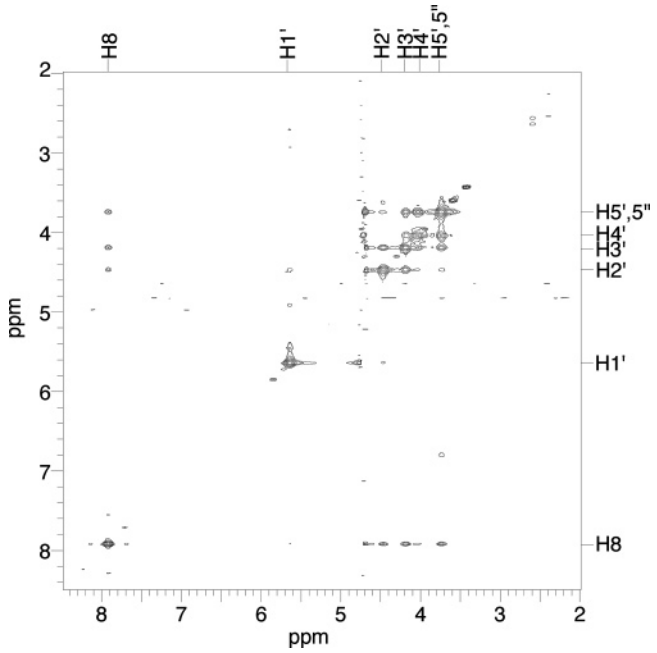

FIGURE 3: Gradient coherence-selected ^{13}C HSQC-TRNOESY of the wild type E·Mg(II)ADP·[U-^{13}C]GMP complex. Conditions: 5 °C, τ_{mix} of 200 ms, 80 transients, 128 increments.

give 4K (F_2) × 1K (F_1) complex point transformed data sets. The use of this isotope-selective technique has the additional benefit in that it readily allows measurement of nOe's for substrate resonances that overlap protein resonances as can be seen by comparison of the ^{13}C-selected TRNOESY spectrum shown in Figure 3 with the ^{1}H TRNOESY spectrum for the E·MgATP complex given in Figure 4.

Theoretical Details. The basic theory of TRNOESY can be found in many publications (*25*−*30*). It has been shown that under fast-exchange conditions, i.e., $\tau_b^{-1}, \tau_f^{-1} \gg (\mathbf{W}_b)_{ij}, (\mathbf{W}_f)_{ij}$, for times greater than $(\tau_b^{-1} + \tau_f^{-1})^{-1}$, the time evolution of the longitudinal magnetizations of an *n*-spin system is given by (*30*)

$$\frac{d}{dt}(\mathbf{m}_b + \mathbf{m}_f) \approx -\mathbf{R}(\mathbf{m}_b + \mathbf{m}_f) \approx -(p_b\mathbf{W}_b + p_f\mathbf{W}_f)(\mathbf{m}_b + \mathbf{m}_f) \quad (2)$$

where the subscripts b and f refer to the bound state and free state, respectively, p_b and p_f are population fractions of

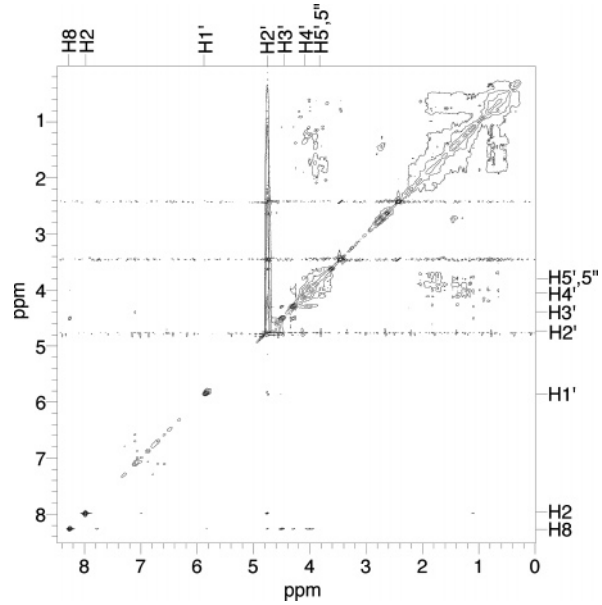

FIGURE 4: TRNOESY of the wild type E·Mg(II)ATP complex. Conditions: 5 °C, τ_{mix} of 160 ms, 16 transients, 256 increments.

the ligand, $\mathbf{m}_b$ and $\mathbf{m}_f$ are *n*-dimensional vectors with each element representing the deviation of the *z*-magnetization of a spin from its equilibrium value, $\mathbf{W}_b$ and $\mathbf{W}_f$ are $n \times n$ relaxation matrices, and τ_b and τ_f are the lifetimes of the bound and free states, respectively. For homonuclear spin systems, if dipolar interaction is the only relaxation mechanism, the relaxation matrix elements of $\mathbf{W}_b$ and $\mathbf{W}_f$ are given by standard expressions (*30*−*33*):

$$\mathbf{W}_{ii} = \frac{\gamma^4\hbar^2\tau_c}{10}\left(1 + \frac{3}{1+\omega^2{\tau_c}^2} + \frac{6}{1+4\omega^2{\tau_c}^2}\right)\sum_{k\neq i} {r_{ik}}^{-6} \quad (3)$$

$$\mathbf{W}_{ij} = \mathbf{W}_{ji} = \frac{\gamma^4\hbar^2\tau_c}{10{r_{ij}}^6}\left(-1 + \frac{6}{1+4\omega^2{\tau_c}^2}\right) \quad (4)$$

where γ and ω are the gyromagnetic ratio and Larmor frequency of the protons, respectively, r_{ij} is the distance between spin *i* and spin *j*, and τ_c is the isotropic rotational correlation time. r_{ij} and τ_c will correspond to free and bound species depending on whether $\mathbf{W}_b$ or $\mathbf{W}_f$ is evaluated. Equations 3 and 4 assume that the spin system is in a single conformation characterized by the distances r_{ij}, and is undergoing isotropic rotational diffusion characterized by τ_c. The intensity of the $i \leftarrow j$ cross-peak in a two-dimensional TRNOESY experiment representing polarization transfer from *j* to *i*, for a mixing time of τ_m, is given by (*1*)

$$m_{i\leftarrow j}(\tau_m) = (e^{-\mathbf{R}\tau_m})_{ij}\mathbf{M}_{0j} = \left[\mathbf{I} - \mathbf{R}\tau_m + \frac{1}{2}\mathbf{R}^2{\tau_m}^2 - \frac{1}{6}\mathbf{R}^3{\tau_m}^3 + ...\right]_{ij}\mathbf{M}_{0j} \quad (5)$$

where $\mathbf{I}$ is the $n \times n$ unit matrix. Equation 5 shows that, for short mixing times, the buildup of intensity of a cross-peak in a TRNOESY spectrum is a polynomial in τ_m, and the initial slope of the buildup curve is given by the linear term $\mathbf{R}_{ij}$. Since usually ${\tau_c}^b \sim 10$ ns, ${\tau_c}^f \sim 0.1$ ns, and $(\omega\tau_c{}^b)^2 \gg 1$, if 10−25% of the ligand is bound so that $p_b \approx 0.1-0.25$, eqs 2 and 4 lead to

$$\mathbf{R}_{ij} \approx p_b(\mathbf{W}_b)_{ij} \approx -\frac{\gamma^4\hbar^2 p_b {\tau_c}^b}{10({r_{ij}^b})^6} \quad (6)$$

Therefore, the ratios of the initial slopes for spin pairs are related to the corresponding internuclear distances in the bound conformation by

$$\frac{\mathbf{R}_{ij}}{\mathbf{R}_{kl}} \approx \left(\frac{r_{kl}^b}{r_{ij}^b}\right)^6 \quad (7)$$

The distance r_{ij}^b can be estimated by using a calibration distance if such a distance can be identified within the spin system. For the nucleotide protons, the H1′−H2′ distance of 2.9 ± 0.2 Å, which remains practically unchanged for all sugar puckers and glycosidic torsions, is a convenient calibration distance and was used in the current work. $p_b\tau_c^b$ may be evaluated from eq 6. It may be seen that the cross-peak intensities in a TRNOESY spectrum for a ligand in fast exchange between bound and free forms are similar to those of an intact system with an effective correlation time given by $p_b\tau_c^b$. Spin diffusion effects are contained in the quadratic and higher-order terms in eq 5 for a system of more than two spins.

Molecular Modeling. Energy minimizations were carried out on a Silicon Graphics Octane computer, running Irix 6.5.17, using SYBYL6.8 from Tripos Inc. (St. Louis, MO). The Tripos force field was used for all energy calculations, and the conjugate gradient algorithm was chosen for the minimization. Partial charges were estimated by the Gasteiger−Marsili method (*34*, *35*) with formal −1 charges assigned to phosphate hydroxyl oxygens and a +2 charge assigned to the divalent cation when it was included in the simulated system. Minimizations of pseudoenergy that included all nOe constraints derived from experimental data (accuracy of ±10%) were performed on MgATP, MgADP, and GMP (including the phosphate groups) in a vacuum with a dielectric constant of 1.

Because H5′ and H5″ coalesce into a single resonance, the observed nOe's with H5′/H5″, such as H8−H5′/H5″, combine contributions from both H5′ and H5″. An average distance can be calculated by taking half the nOe buildup rate. If spin *i* has distances r_{i1} and r_{i2} from H5′ and H5″, respectively, this average distance, r_{iavg}, is related to r_{i1} and r_i by

$$r_{iavg} = \left(\frac{{r_{i1}}^{-6} + {r_{i2}}^{-6}}{2}\right)^{-1/6} \quad (8)$$

Except for the special case in which $r_{i1} = r_{i2}$, r_{iavg} does not equal the distance from spin *i* to either H5′ or H5″. However, if $r_{i1} < r_{i2}$, we have $r_{i1} < r_{iavg} < r_{i2}$. Although r_{i1} and r_{i2} cannot be specified explicitly, their upper and lower bounds are limited by the maximum distance for observable nOe's, ∼5 Å (barring unusual spin diffusion effects), and by twice the van der Waals radius of protons, ∼1.8 Å. Therefore, in molecular modeling calculations, the 1.8 Å $< r_{i1} < r_{iavg} < r_{i2} <$ 5 Å model was used as a general constraint for H5′

Table 1: Interproton Distance Constraints for Adenosine Determined from Analyses of TRNOESY Data of Wild Type and Y78F Mutant GKy in E·MgATP Complexes

	wild type		Y78F mutant	
distance	measured (±10%)	model (±0.3 Å)	measured (±10%)	model (±0.3 Å)
H8−H1′	3.7	3.4	3.5	3.5
H8−H2′	2.7	2.7	2.2	2.3
H8−H3′	3.5	3.3	3.1	3.4
H8−H4′	3.2	3.7	3.5	3.7
H8−H5′	3.4[a]	2.8	3.4[a]	2.3
H8−H5″	*a*	3.5	*a*	3.5
H1′−H2′	2.9	2.9	2.9	2.9
H1′−H3′	3.3	3.7	3.5	3.6
H1′−H4′	3.1	2.8	3.8	3.6
H1′−H5′	3.9[a]	3.7	4.1[a]	4.3
H1′−H5″	*a*	4.6	*a*	5.0
χ (O4′−C1′−N9−C8)		54 ± 5°		55 ± 5°

[a] This distance represents a nonlinear average of the two nOe interactions (see the text).

Table 2: Interproton Distance Constraints for Adenosine Determined from Analyses of TRNOESY Data of Wild Type and Y78F Mutant GKy in E·MgADP Complexes

	wild type		Y78F mutant	
distance	measured (±10%)	model (±0.3 Å)	measured (±10%)	model (±0.3 Å)
H8−H1′	3.7	3.4	4.1	3.3
H8−H2′	2.7	2.6	2.3	2.4
H8−H3′	3.4	3.4	3.2	3.1
H8−H4′	2.9	3.4	2.6	3.1
H8−H5′	3.5[a]	3.1	3.0[a]	2.2
H8−H5″	*a*	3.4	*a*	2.6
H1′−H2′	2.9	2.9	2.9	2.9
H1′−H3′	3.2	3.6	3.7	3.8
H1′−H4′	2.8	2.4	2.8	2.5
H1′−H5′	3.6[a]	3.8	4.0[a]	4.6
H1′−H5″	*a*	4.4	*a*	3.7
χ (O4′−C1′−N9−C8)		53 ± 5°		51 ± 5°

[a] This distance represents a nonlinear average of the two nOe interactions (see the text).

and H5″ nOe's in which r_{i1} always represented the shorter of the two distances from spin *i* to H5′/H5″.

RESULTS AND ANALYSIS

TRNOESY experiments were performed on E·Mg(II)·ATP, E·Mg(II)·ADP, and E·GMP complexes of both wild type and Y78F mutant GKy. Gradient coherence-selected ^{13}C HSQC-TRNOESY experiments were performed on E·Mg(II)·ADP·[U-^{13}C]GMP complexes of both wild type and Y78F mutant GKy. Sample conditions for the experiments appropriate for minimizing effects from nonspecific binding were determined with a preliminary study of concentration effects on nOe at a 120 ms mixing time over the range of 1−3 mM nucleotide at a 10:1 ligand:enzyme concentration. The narrow range was deliberately chosen on the basis of results of such studies with other enzymes that indicate that nonspecific binding has a K_D of >4 mM (*1*−*4*, *6*). On the basis of this preliminary study of sample conditions, subsequent samples contained 0.3 mM enzyme and 3 mM nucleotide, or nucleotides in the case of the two substrate complexes measured by gradient coherence-selected ^{13}C HSQC-TRNOESY.

Intramolecular nOe's of Adenyl-Nucleotides in Wild Type and Y78F Mutant GKy-Bound Complexes. The H8−H2′ cross-peak was the strongest adenyl-nucleotide nOe cross-peak in 2D TRNOESY spectra of GKy-bound adenyl-nucleotide. This indicates that these adenyl-nucleotides bind in the anti conformation. nOe buildups from nucleotide nOe's separable from the background protein intramolecular nOe's were used as constraints in molecular dynamics modeling. In all cases, nOe's between either H8 or H1′ and each of the sugar protons were outside the protein background. The buildups of their nOe's were readily measurable and could provide distance constraints. Of course, overlapping cross-peaks occur for H8−H5′ and H8−H5″, as well as for H1′−H5′ and H1′−H5″.

Table 1 shows distances computed from TRNOESY data and distances fitted by molecular dynamics for both wild type and Y78F GKy complexes with MgATP. The interproton distances for the model are averaged over 11 structures deemed acceptable on the basis of agreement with experimental data. For the MgATP data, the major violations occur for the H8−H5′ and H8−H5″ distances. The data for Y78F yielded a better fit than the wild type. The rmsd values for the distance data (ignoring H8−H5′ and H8−H5″) are 0.39 Å for the wild type and 0.29 Å for Y78F. The rmsd of the glycosidic torsion is 2.5° for the wild type and 2.3° for Y78F, while the rmsd for the dihedral angles of the sugar was 20.0° for the wild type and 5.4° for Y78F.

The wild type and Y78F mutant bind MgATP equally well, and the mutation is at the putative GMP binding site. Therefore, one might expect the bound conformations of MgATP to be similar. In the energy minimization fit, the major difference in conformations is related to the C4′−C5′ sugar dihedral angle, γ. Although this angle is only constrained by the H8−H5′,5″ and H1′−H5′,5″ nOe data, the difference might represent a real difference in the orientation of the phosphate chain in the respective complexes. The glycosidic angle, χ, however, is constrained well by the nOe data, and the fact that it is identical in the two complexes points to the sugar and base being bound very similarly in the respective complexes.

The sugar puckers computed by molecular modeling, shown for the two complexes in columns 2 and 6 of Table 4, are different. On the basis of models of deoxynucleotides, it was shown that the dihedral angles determining sugar pucker are not particularly sensitive to ribose interproton distances other than H3′−H4′ and H1′−H4′ (*36*). In our experiments, only the H1′−H4′ distance gives a cross-peak separable from the protein background, and the calculated distances are significantly different. This difference as well as the differences in some of the distances involving H8 indicates that the details of sugar pucker may be different in the two complexes. However, in view of the large rmsd values for the dihedral angles, differences in the values of the actual parameters used to characterize sugar pucker, *P* and α, are not likely to be accurate enough to be interpretable.

Table 2 shows distances computed from TRNOESY data and distances fitted by molecular dynamics for wild type and Y78F guanylate kinase complexes with MgADP. As was the case with MgATP, both variants bind MgADP equally well, and the structures of the respective MgADP complexes are similar as well. The average rmsd values for distance data (ignoring distances involving 5′ and 5″ protons as above)

are 0.34 Å for the wild type and 0.23 Å for the mutant. The rmsd values for the ribose dihedral angles are in the range of 12−14° in the two cases, and are in the range of 1.3−1.6° for the glycosidic torsion. As described above, the major difference in conformations is likely to be related to the orientation of the phosphate chain with respect to the base and the sugar. Also as expected, the glycosidic angles, χ, which were well-constrained in the two complexes, are similar. Again, there are differences in the computed sugar puckers as given in columns 3 and 7 of Table 4, but the same limitation as noted above applies here as well.

GMP Complexes with Wild Type and Y78F Mutant GKy. TRNOESY measurements were first made on binary complexes of wild type and Y78F guanylate kinase with GMP. Distances computed from the data and fitted by molecular dynamics (data not shown) indicate that the two structures are similar. The following reasoning, however, suggested that this result may not guarantee conformational invariance of GMP at its site despite the mutation. It is important to note that in addition to ATP, guanylate kinase can use GTP as the phosphate source. Thus, both nucleotide binding sites are able to bind GMP. Furthermore, since the kinetic affinity of GMP with the Y78F mutant is reduced by a factor of 20 relative to that for the wild type enzyme, the data for the binary GMP complex of Y78F may primarily represent binding at the adenyl site. Therefore, to address the question of whether the mutation affects the conformation of GMP bound at its site, it became imperative to block the adenyl site for GMP. For this purpose, MgADP was added to the sample containing the enzyme and GMP. Unfortunately, sugar resonances for the two nucleotides overlap in E·MgADP·GMP complexes. Therefore, an isotope selective nOe experiment was devised to resolve the signals.

MgADP·[U-^{13}C]GMP Complexes with Wild Type and Y78F Mutant GKy. Isotope-selective nOe allows selection of the nOe resonances to be observed. In the case of this complex, proton resonances from MgADP are not observed. An additional benefit to this experiment was the ability to measure cross-peaks between all of the proton pairs of GMP because the isotope selection suppressed the background resonances from the protein. Thus, more constraints were generated for bound GMP in these complexes. Table 3 shows distances computed from TRNOESY data and distances fitted by molecular dynamics for [U-^{13}C]GMP in wild type and Y78F guanylate kinase complexes with MgADP·[U-^{13}C]-GMP. Eleven acceptable structures were used to compute averaged distance data given in Table 3. The availability of more comprehensive nOe data helped to obtain a better agreement between the pseudo-energy minimization model and the experimentally determined distances (than for the MgATP or MgADP complexes) with violations primarily involving 5′ and 5″ protons. The average rmsd values for distance data are 0.24 Å for the wild type and 0.3 Å for Y78F. The corresponding values for the ribose dihedral angles were 9.5° for the wild type and 1.3° for Y78F. The rmsds for the glycosidic torsion were 2.5° for the wild type and 0.5° for Y78F.

The conformations of bound GMP are different for the two proteins. There is very good convergence between the glycosidic torsion angles in the pseudo-energy minimization ensembles. The point mutation has resulted in the guanine base binding with an unusual glycosidic angle of 83 ± 5° in the Y78F mutant E·MgADP·GMP complex. Figure 5 gives a comparison of the orientations of the base in the wild type and Y78F mutant complexes. The relative orientation of Y78F and GMP revealed by X-ray crystallography of the wild type E·GMP complex (*18*) is shown in Figure 6 with the Y78−GMP phosphate hydrogen bond indicated. The weakening of GMP binding to Y78F by more than 1 order of magnitude relative to that of the wild type would be related in part to the absence of this hydrogen bond. The molecular dynamics fit of the TRNOESY data reveals that the reduction in affinity is accompanied by a significant change in the glycosidic torsion. Mean values of sugar ring torsion angles and pseudorotation parameters obtained for GMP in the E·MgADP·GMP complex for both wild type and Y78F mutant are given in Table 4 along with those for the other complexes studied. Because the isotope-filtered data were allowed to be measured for all GMP ribose proton pairs, including those for H3′−H4′ and H1′−H4′, the GMP ribose puckers for these complexes were each subject to all possible distance

Table 3: Interproton Distance Constraints for Guanosine Determined from Analyses of TRNOESY Data of Wild Type and Y78F Mutant GKy in E·MgADP·[U-^{13}C]GMP Complexes

	wild type		Y78F mutant	
distance	measured (±10%)	model (±0.3 Å)	measured (±10%)	model (±0.3 Å)
H8−H1′	3.1	3.5	3.3	3.7
H8−H2′	2.2	2.1	2.6	2.2
H8−H3′	2.9	3.3	2.4	2.7
H8−H4′	4.1	3.9	3.6	4.1
H8−H5′	3.8[a]	2.4	2.8[a]	2.0
H8−H5″	*a*	3.8	*a*	3.8
H1′−H2′	2.9	2.9	2.9	2.8
H1′−H3′	3.4	3.8	3.7	4.2
H1′−H4′	3.1	3.0	3.2	3.5
H1′−H5′	*b*	4.4	3.7[a]	3.7
H1′−H5″	*b*	4.5	*a*	4.4
H2′−H3′	2.0	2.0	1.9	2.0
H2′−H4′	2.8	3.3	2.8	3.3
H2′−H5′	2.9[a]	3.0	2.8[a]	3.0
H2′−H5″	*a*	4.2	*a*	4.3
H3′−H4′	2.2	2.5	2.2	2.5
H3′−H5′	2.7[a]	2.5	2.5[a]	2.4
H3′−H5″	*a*	3.4	*a*	3.4
H4′−H5′	2.2[a]	2.9	2.1[a]	2.6
H4′−H5″	*a*	2.3	*a*	2.2
χ (O4′−C1′−N9−C8)		50 ± 5°		83 ± 5°
χ (X-ray)[c]		90 ± 5°		*d*

[a] This distance represents a nonlinear average of the two nOe interactions (see the text). [b] Not detected. [c] Measured for the E·GMP complex (*18*, *19*). [d] Structure not available.

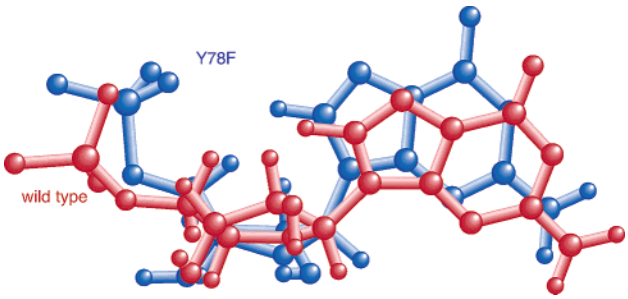

FIGURE 5: Comparison of conformations of GMP in the E·MgADP·GMP complex for wild type (red) and Y78F mutant (blue) GKy. Each of the structures drawn represents one of 11 acceptable structures obtained for the respective complex by energy minimization.

Table 4: Mean Values (in degrees, ±5°) of Various Torsion[a] Angles and Pseudorotation[b] Parameters of the Sugar Ring in the Calculated Structural Ensembles of GKy-Bound Nucleotides

	wild type				Y78F mutant			
angle	E·MgATP	E·MgADP	E·GMP	E·MgADP·[U-^{13}C]GMP[c]	E·MgATP	E·MgADP	E·GMP	E·MgADP·[U-^{13}C]GMP[c]
χ	54	53	54	50	55	51	50	83
ν_0	8	−4	30	−17	−3	6	5	34
ν_1	1	16	−28	25	21	9	6	−30
ν_2	−9	−20	19	−21	−29	−19	−16	11
ν_3	15	21	0	12	28	24	19	13
ν_4	−14	−11	−21	3	15	−20	14	−32
P	107	172	159	153	193	215	214	−73
a	18	19	30	24	30	23	19	37

[a] Torsions are denoted as follows: χ, O4′−C1′−N9−C8; ν_0, C4′−O4′−C1′−C2′; ν_1, O4′−C1′−C2′−C3′; ν_2, C1′−C2′−C3′−C4′; ν_3, C2′−C3′−C4′−O4′; ν_4, C3′−C4′−O4′−C1′. [b] P {$=\tan^{-1}[(\nu_4 + \nu_1) - (\nu_3 + \nu_0)/2\nu_2(\sin 36° + \sin 72°)]$} and α ($=\nu_2/\cos P$) are the phase angle and amplitude of pseudorotation of the sugar ring, respectively. When ν_2 is negative, 180° is added to the calculated value of P. [c] [U-^{13}C]GMP used in a ^{13}C-selective TRNOESY experiment to observe GMP resonances in the presence of overlapping resonances from unlabeled ADP.

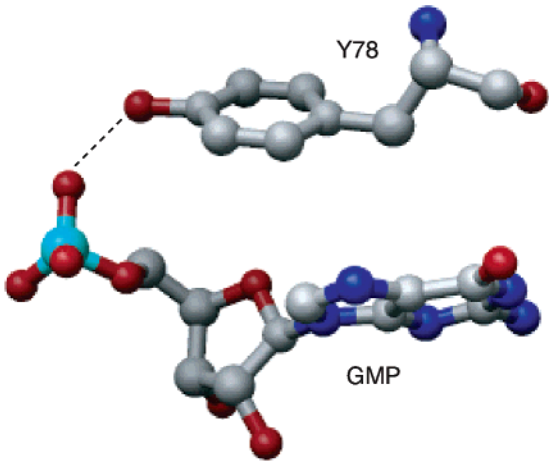

FIGURE 6: Relative location of Y78 and GMP as revealed by X-ray crystallography (*19*). The Y78 hydroxyl−GMP phosphate hydrogen bond is labeled. This figure was produced using the UCSF Chimera package from the Computer Graphics Laboratory, University of California, San Francisco, CA (supported by NIH Grant P41 RR-01081) (*37*).

constraints, in comparison with the ATP and ADP complexes, and the sugar pucker parameters for GMP complexes are more accurate (shown in columns 5 and 9 of Table 4). However, it is not clear if the differences in sugar pucker between the wild type and mutant complexes are interpretable. Finally, it may be noted that the guanyl χ value for the wild type E·MgADP·GMP complex (50 ± 5°) is significantly different from the value of 90 ± 5° determined from the X-ray structure of wild type GKy·GMP complex (*18*, *19*).

DISCUSSION

The results of this paper are aimed at investigating how mutation of an active site amino acid residue, deemed to be critical for the reaction, might alter the conformation of substrates or reaction complexes bound to the enzyme. The criticality of an amino acid residue is typically deduced initially on the basis of measurements of substrate binding affinities and of enzyme activity. While a severe reduction in these parameters is a clear pointer for the importance of the specific residue in the mechanism of the overall reaction, the manner in which such changes are manifested may be understood in structural terms by investigating the structural alterations of the bound substrates as well as of the residues at the active site. In the case of enzymes utilizing nucleotides as substrates, comprehensive NMR methodologies making use of measurements of TRNOESY and paramagnetic relaxation enhancements for ^{31}P and ^{13}C nuclei in the substrates have yielded structural data for enzyme-bound nucleotides (*6*, *38*). The NMR structures often differ from those determined by X-ray crystallography. However, since the NMR data were obtained in solution, they are considered reliable for the bound substrates while the crystallography data are usually the only source of structural data for their amino acid environment (*38*).

Wild type and Y78F mutant GKy offer a good case for this investigation. Evidence for the role of Y78 in binding GMP at its site was obtained from both binding and kinetic data, while the corresponding structural data related to bound GMP conformation were not yet available. The results presented in this paper are on the adenosine (MgATP and MgADP) and guanosine (GMP) conformations based on proton TRNOESY measurements. The experiments on the adenosine nucleotides can be performed with their binary complexes with the enzyme. On the other hand, since the enzyme can also use GTP in place of ATP, in order to make measurements on GMP bound at its binding site, the other site was blocked for GMP through the addition of MgADP to the complex. This procedure, in turn, produced a NMR technical difficulty as the ribose resonances of ADP and GMP overlapped. A ^{13}C-filtered TRNOESY method was devised to overcome this problem by utilizing [U-^{13}C]GMP as a substrate. Thus, MgADP serves the purpose of blocking the binding of GMP at the ATP site, but its resonances are not seen in the spectrum. This method generated an added advantage eliminating the protein background in the spectrum as well, thereby allowing nOe measurements of all sugar proton pairs of GMP.

The adenosine conformations obtained for Mg(II)ATP and for Mg(II)ADP bound either to wild type or to Y78F mutant GKy have glycosidic torsion angles between 49 ± 5° and 55 ± 5°, in good agreement with the range of 52 ± 8° previously reported for a number of ATP-utilizing enzymes (*1*−*6*). It should first be noted that the mutation does not affect the adenosine conformation, consistent with the fact that the pertinent residue is implicated in GMP binding. Furthermore, this result is consistent with the observation made earlier that this glycosidic orientation appears to be a productive structural motif for adenine nucleotides (*4*, *6*). This feature could not be detected in published X-ray

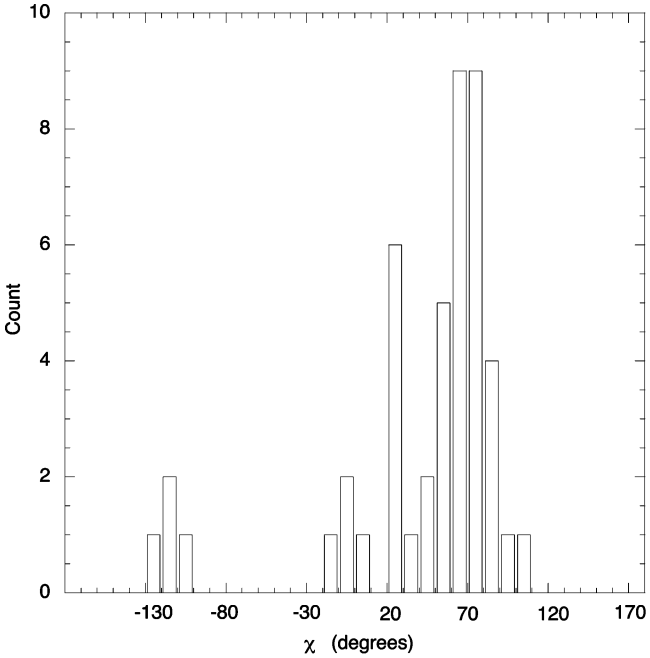

FIGURE 7: Histogram of glycosidic torsion angles (χ) measured from X-ray structures of guanine nucleotide complexes of various guanine nucleotide-utilizing enzymes (data collected from references given in the Supporting Information).

structures in which values of χ ranged from $-170°$ to $180°$ (*6*).

The glycosidic torsion angle for GMP (χ) in the wild type E·MgADP·[U-^{13}C]GMP complex is determined to be $50 \pm 5°$. This value is in the same range given above for the adenosine conformations for a number of enzymes. However, to the best of our knowledge, this χ value is the only one so far determined for enzyme-bound guanine nucleotides by NMR, and therefore, it is premature to attach any significance to its being in the same range. Nevertheless, it may be noted in this context that a search of published X-ray structures involving enzyme-bound 5′-guanosine nucleotides also revealed a broad range of values for χ similar to the X-ray data for adenosine conformations. A histogram of these data is shown in Figure 7. Further NMR determinations of χ for more enzyme-bound guanine nucleotides may indicate whether a narrow range will be found in the solution phase for guanosine conformations as well, thereby pointing to a productive structural motif similar to that for adenine nucleotides.

It may be noted that the guanyl glycosidic torsion angle in the X-ray structure of E·GMP (*18*, *19*) is $90 \pm 5°$, significantly outside the experimental error for the NMR value of $50 \pm 5°$. The pattern of differences in this structural parameter as measured by the two methods continues. The two structures are pictorially compared in Figure 8. It is evident the crystallization often traps the nucleotide in an unfavorable glycosidic orientation.

The result that is most directly pertinent to the motivation of this investigation is that the glycosidic torsion of GMP in the E·MgADP·[U-^{13}C]GMP complex of Y78F is found to be $83 \pm 5°$, strikingly different from the value of $50 \pm 5°$ in the complex for wild type GKy. This change directly links the structural alteration accompanying the diminished binding affinity of GMP by a factor of 30, as well as to the reduction in enzymatic activity by 2 orders of magnitude.

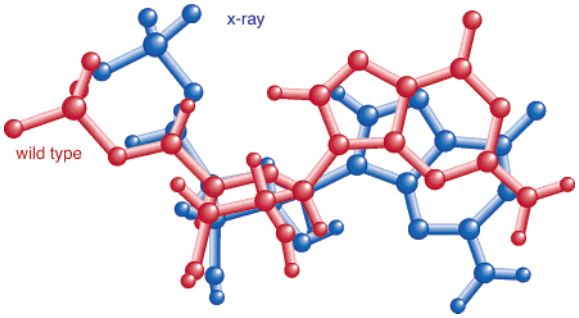

FIGURE 8: Comparison of conformations of GMP bound to wild type GKy as measured by NMR in the E·MgADP·GMP complex (red) and by X-ray in the E·GMP complex (blue). The wild type structure is the same as that in Figure 5, and the X-ray structure is the same as that of GMP in Figure 6.

The following features of sequence and structural data are relevant to distinguishing the wild type and Y78F mutants in their GMP binding. In the wild type GKy sequence, residues 77 and 78 are both tyrosines. Crystal structure data on the wild type protein·GMP complex show that hydroxyl groups of Y78 and Y50 may be hydrogen bonded to the phosphate of GMP (*17*−*19*). Published nOe data indicate that F78 occupies the same spatial position in Y78F as Y78 does in the wild type protein. Previous studies of the related enzyme, adenylate kinase, did not reveal intermolecular nOe's between ATP or ADP and any of the protein resonances in the aromatic region (*6*, *23*). This appears to be true for ATP, for ADP, and for GMP bound to either wild type or Y78F mutant GKy as well. The absence of these nOe's shows that, barring unusual spin diffusion effects, the distances between the nonexchangeable proton of the guanosine moiety and those of the proximal residues of the protein are likely exceed a rule of thumb distance of 5 Å in both forms of the protein. Thus, the large and unmistakable change in χ of GMP does not seem to be directly linked either to the excising of one of the hydrogen bonds (from Y78) or to major protein conformational changes. Further understanding of such structural alterations in enzyme-bound reaction complexes is likely to emerge as more data of this kind are obtained.

ACKNOWLEDGMENT

Thanks are due to Ms. Marina Lyshevski and Mr. Joshua Scott of the NMR group.

SUPPORTING INFORMATION AVAILABLE

A table showing glycosidic torsion angles, χ, measured for enzyme-bound guanyl-nucleotides from X-ray structures available in the Protein Data Bank up to April 2005. This material is available free of charge via the Internet at http://pubs.acs.org.

REFERENCES

1. Murali, N., Jarori, G. K., Landy, S. B., and Nageswara Rao, B. D. (1993) Two-Dimensional Transferred Nuclear Overhauser Effect Spectroscopy (TRNOESY) Studies of Nucleotide Conformations in Creatine Kinase Complexes: Effects Due to Weak Nonspecific Binding, *Biochemistry 32*, 12941−12948.
2. Murali, N., Jarori, G. K., and Nageswara Rao, B. D. (1994) Two-Dimensional Transferred Nuclear Overhauser Effect Spectroscopy Study of the Conformation of MgATP Bound at the Active and

Ancillary Sites of Rabbit Muscle Pyruvate Kinase, *Biochemistry 33*, 14227−14236.
3. Jarori, G. K., Murali, N., and Nageswara Rao, B. D. (1994) Two-Dimensional Transferred Nuclear Overhauser Effect Spectroscopy (TRNOESY) Studies of Nucleotide Conformations in Arginine Kinase Complexes, *Biochemistry 33*, 6784−6791.
4. Murali, N., Lin, Y., Mechulam, Y., Plateau, P., and Nageswara Rao, B. D. (1997) Adenosine Conformations of Nucleotides Bound to Methionyl tRNA Synthetase by Transferred Nuclear Overhauser Effect Spectroscopy, *Biophys. J. 70*, 2275−2284.
5. Jarori, G. K., Murali, N., Switzer, R. L., and Nageswara Rao, B. D. (1995) Conformation of MgAtp Bound to 5-Phospho-α-D-Ribose 1-Diphosphate Synthetase by Two-Dimensional Transferred Nuclear Overhauser Effect Spectroscopy, *Eur. J. Biochem. 230*, 517−524.
6. Lin, Y., and Nageswara Rao, B. D. (2000) Structural Characterization of Adenine Nucleotides Bound to *Escherichia coli* Adenylate Kinase. 1. Adenosine Conformations by Proton Two-Dimensional Transferred Nuclear Overhauser Spectroscopy, *Biochemistry 39*, 3636−3646.
7. Berger, A., Schiltz, E., and Schulz, G. E. (1989) Guanylate Kinase from *Saccharomyces cerevisiae*: Isolation and Characterization, Crystallization and Preliminary X-ray Analysis, Amino Acid Sequence and Comparison with Adenylate Kinases, *Eur. J. Biochem. 184*, 433−443.
8. Li, Y., Zhang, Y., and Yan, H. (1996) Kinetic and Thermodynamic Characterizations of Yeast Guanylate Kinase, *J. Biol. Chem. 271*, 28038−28044.
9. Hall, S. W., and Kühn, H. (1986) Purification and Properties of Guanylate Kinase from Bovine Retinas and Rod Outer Segments, *Eur. J. Biochem. 161*, 551−556.
10. Miller, R. L., and Miller, W. H. (1980) Phosphorylation of Acyclovir (Acycloguanosine) Monophosphate by GMP Kinase, *J. Biol. Chem. 255*, 7204−7207.
11. Boehme, R. E. (1984) Phosphorylation of the Antiviral Precursor 9-(1,3-Dihydroxy-2-propoxymethyl)guanine Monophosphate by Guanylate Kinase Isozymes, *J. Biol. Chem. 259*, 12346−12349.
12. Miller, W. H., Daluge, S. M., Garvey, E. P., Hopkins, S., Reardon, J. E., Boyd, F. L., and Miller, R. L. (1992) Phosphorylation of Carbovir Enantiomers by Cellular Enzymes Determines the Stereoselectivity of Antiviral Activity, *J. Biol. Chem. 267*, 21220−21224.
13. Woods, D. F., and Bryant, P. J. (1991) The Discs-Large Tumor Suppressor Gene of *Drosophila* Encodes a Guanylate Kinase Homolog Localized at Septate Junctions, *Cell 66*, 451−464.
14. Kistner, U., Wenzel, B. M., Veh, R. W., Cases-Langhoff, C., Garner, A. M., Appeltauer, U., Voss, B., Gundelfinger, E. D., and Garner, C. C. (1993) SAP90, a Rat Presynaptic Protein Related to the Product of the *Drosophila* Tumor Suppressor Gene *dlg*A, *J. Biol. Chem. 268*, 4580−4583.
15. Cho, K.-O., Hunt, C. A., and Kennedy, M. B. (1992) The Rat Brain Postsynaptic Density Fraction Contains a Homolog of the *Drosophila* Discs-Large Tumor Suppressor Protein, *Neuron 9*, 929−942.
16. Bryant, P. J., and Woods, D. F. (1992) A Major Palmitoylated Membrane Protein of Human Erythrocytes Shows Homology to Yeast Guanylate Kinase and to the Product of a *Drosophila* Tumor Suppressor Gene, *Cell 68*, 621−622.
17. Stehle, T., and Schulz, G. E. (1990) Three-dimensional Structure of the Complex of Guanylate Kinase from Yeast with its Substrate GMP, *J. Mol. Biol. 211*, 249−254.
18. Stehle, T., and Schulz, G. E. (1992) Refined Structure of the Complex between Guanylate Kinase and its Substrate GMP at 2.0 Å Resolution, *J. Mol. Biol. 224*, 1127−1141.
19. Blaszczyk, J., Li, Y., Yan, H., and Ji, X. (2001) Crystal Structure of Unligated Guanylate Kinase from Yeast Reveals GMP-induced Conformational Changes, *J. Mol. Biol. 307*, 242−257.
20. Zhang, Y., Li, Y., Wu, Y., and Yan, H. (1997) Structural and Functional Roles of Tyrosine 78 of Yeast Guanylate Kinase, *J. Biol. Chem. 272*, 19343−19350.
21. Agarwal, K. C., Miech, R. P., and Parks, R. E., Jr. (1978) Guanylate Kinases from Human Erythrocytes, Hog Brain, and Rat Liver, *Methods Enzymol. 51*, 483−490.
22. States, D. J., Haberkorn, R. A., and Ruben, D. J. (1982) A Two-Dimensional Nuclear Overhauser Experiment with Pure Absorption Phase in Four Quadrants, *J. Magn. Reson. 48*, 286−292.
23. Vetter, I. R., Reinstein, J., and Rösch, P. (1990) Complexes of *Escherichia coli* Adenylate Kinase and Nucleotides: Proton NMR Studies of the Nucleotide Sites in Solution, *Biochemistry 29*, 7459−7467.
24. Wagner, R., and Berger, S. (1997) Heteronuclear Edited Gradient Selected 1D and 2D NOE Spectra: Determination of the NOE Effect between Chemically Equivalent Protons, *Magn. Reson. Chem. 35*, 199−202.
25. Campbell, A. P., and Sykes, B. D. (1991) Theoretical Evaluation of the Two-Dimensional Transferred Nuclear Overhauser Effect, *J. Magn. Reson. 93*, 77−92.
26. Ni, F. (1992) Complete Relaxation Matrix Analysis of Transferred Nuclear Overhauser Effects, *J. Magn. Reson. 96*, 651−656.
27. Lee, W., and Krishna, N. R. (1992) Influence of Conformational Exchange on the 2D NOESY Spectra of Biomolecules Existing in Multiple Conformations, *J. Magn. Reson. 98*, 36−48.
28. London, R. E., Perlman, M. E., and Davis, D. G. (1992) Relaxation-Matrix Analysis of the Transferred Nuclear Overhauser Effect for Finite Exchange Rates, *J. Magn. Reson. 97*, 79−98.
29. Zheng, J., and Post, C. B. (1993) Protein Indirect Relaxation Effects in Exchange-Transferred NOESY by a Rate-Matrix Analysis, *J. Magn. Reson., Ser. B 101*, 262−270.
30. Landy, S. B., and Nageswara Rao, B. D. (1989) Dynamical NOE in Multiple-Spin Systems Undergoing Chemical Exchange, *J. Magn. Reson. 81*, 371−377.
31. Abragam, A. (1961) *Principles of Nuclear Magnetism*, Oxford University Press, London.
32. Noggle, J. H., and Schirmer, R. E. (1971) *The Nuclear Overhauser Effect*, Academic Press, New York.
33. Keepers, J. W., and James, T. L. (1984) A Theoretical Study of Distance Determinations From NMR: Two-Dimensional Nuclear Overhauser Effect Spectra, *J. Magn. Reson. 57*, 404−426.
34. Gasteiger, J., and Marsili, M. (1980) Iterative Partial Equalization of Orbital Electronegativity: A Rapid Access To Atomic Charges, *Tetrahedron 36*, 3219−3228.
35. Marsili, M., and Gasteiger, J. (1980) Pi-Charge Distributions from Molecular Topology and Pi-Orbital Electronegativity *Croat. Chem. Acta 53*, 601−614.
36. Hosur, R. V., Govil, G., and Miles, H. T. (1988) Application of 2D NMR Spectroscopy in the Determination of Solution Conformation of Nucleic Acids, *Magn. Reson. Chem. 26*, 927−944.
37. Pettersen, E. F., Goddard, T. D., Huang, C. C., Couch, G. S., Greenblatt, D. M., Meng, E. C., and Ferrin, T. E. (2004) UCSF Chimera: A Visualization System for Exploratory Research and Analysis, *J. Comput. Chem. 25*, 1605−1612.
38. Lin, Y., and Nageswara Rao, B. D. (2000) Structural Characterization of Adenine Nucleotides Bound to *Escherichia coli* Adenylate Kinase. 2. ^{31}P and ^{13}C Relaxation Measurements in the Presence of Cobalt(II) and Manganese(II), *Biochemistry 39*, 3647−3655.
39. Ray, B. D., Jarori, G. K., and Nageswara Rao, B. D. (2002) Quantitation of Movement of the Phosphoryl Group During Catalytic Transfer in the Arginine Kinase Reaction: ^{31}P Relaxation Measurements on Enzyme-Bound Equilibrium Mixtures, *J. Biomol. NMR 23*, 13−21.

BI0509088